Structure of Daidzin, a Naturally Occurring Anti-Alcohol-Addiction Agent, in Complex with Human Mitochondrial Aldehyde Dehydrogenase[§]

Edward D. Lowe,*[,†] Guang-Yao Gao,[‡] Louise N. Johnson,[†] and Wing Ming Keung[‡,#]

Laboratory of Molecular Biophysics, University of Oxford, Rex Richards Building, Oxford OX1 3QU, U.K., and Department of Pathology and Centre for Biochemical and Biophysical Sciences and Medicine, Harvard Medical School, 77 Avenue Louis Pasteur, Boston, Massachusetts, 02115

Received January 21, 2008

The *ALDH2*2* gene encoding the inactive variant form of mitochondrial aldehyde dehydrogenase (ALDH2) protects nearly all carriers of this gene from alcoholism. Inhibition of ALDH2 has hence become a possible strategy to treat alcoholism. The natural product 7-*O*-glucosyl-4′-hydroxyisoflavone (daidzin), isolated from the kudzu vine (*Peruraria lobata*), is a specific inhibitor of ALDH2 and suppresses ethanol consumption. Daidzin is the active principle in a herbal remedy for "alcohol addiction" and provides a lead for the design of improved ALDH2. The structure of daidzin/ALDH2 in complex at 2.4 Å resolution shows the isoflavone moiety of daidzin binding close to the aldehyde substrate-binding site in a hydrophobic cleft and the glucosyl function binding to a hydrophobic patch immediately outside the isoflavone-binding pocket. These observations provide an explanation for both the specificity and affinity of daidzin (IC_{50} = 80 nM) and the affinity of analogues with different substituents at the glucosyl position.

Introduction

Aldehyde dehydrogenases (ALDHs[a]) are a family of NAD^+ ($NADP^+$) dependent enzymes that catalyze the oxidation of endogenous and exogenous aldehydes[1–4] (e.g., acetaldehyde + NAD^+ → acetate + NADH). The most abundant and best studied are the cytosolic (ALDH1) and mitochondrial isozymes (ALDH2). They are tetrameric proteins with subunits comprising 499 (ALDH1) or 500 (ALDH2) amino acids and share 68% sequence identity. The enzymes catalyze the oxidation of acetaldehyde (AcH), but ALDH2 is the more efficient[5] and is important in the oxidative elimination of AcH after consuming ethanol. Numerous genetic predisposing factors have been implicated for or against alcoholism.[6,7] The *ALDH2*2* gene encoding the inactive variant form of ALDH2 (E487K mutant) is common among East Asians. On consumption of alcohol, subjects carrying this inactive variant exhibit high levels of blood AcH giving rise to flushes in heterozygotes and more severe reactions in homozygotes.[8] These effects exert discomfort, and they deter almost all carriers of this gene from alcohol abuse and alcoholism.[9–11] Individuals who have inherited this null *ALDH2*2* gene do not suffer from any physiological abnormality except for a compromised capacity to metabolize acetaldehyde (AcH).[12,13] ALDH2 has therefore been considered a target for the treatment of alcoholism. In support of this approach Ocaranza et al.[14] have shown that inhibiting the expression of the ALDH2 gene in alcohol-addicted rats by an antisense anti-ALDH2 gene carried by an adenoviral vector curtailed the drive of rats to consume alcohol.

Antabuse (disulfiram, DS, tetraethylthiuram disulfide), the first drug to be developed for the treatment of alcoholism,[15] is principally an inhibitor of ALDH1 and covalently modifies sulfydryl groups at the catalytic site.[16] In vitro, DS is a less effective inhibitor of ALDH2,[17] but in vivo studies have demonstrated that a metabolite of DS inhibits ALDH2 by carbomoylation at Cys302.[18] DS also inhibits a number of other enzymes critical in drug, xenobiotic, neurotransmitter, and intermediary metabolism leading to unwanted side effects.[16] Supervised and carefully scheduled, DS is useful in the treatment of alcoholism as are other approved drugs such as naltrexone, which blocks opioid receptors preventing the euphoric effects of alcohol, and acamprosate, which inhibits glutamate signaling and is thought to reduce withdrawal symptons.[19–21] However, there is a considerable need for improved drugs together with better understanding of other factors, including genetic effects, that influence addiction to alcohol (summarized in ref 22).

Daidzin (7-*O*-glucosyl-4′-hydroxyisoflavone) is a potent, reversible, and selective inhibitor of ALDH2.[17,23] It reduces ethanol consumption in all ethanol drinking animal models tested to date.[23–26] There have been indications that daidzin inhibition of ALDH2 exerts effects on other aldehyde pathways that are distinct from AcH metabolism. Daidzin reduces ethanol consumption in Syrian golden hamsters, where AcH can be metabolized by other enzymes and ALDH2 is not essential.[27] The monoamine oxidase (MAO)/ALDH2 pathway has been identified as a potential site of action in isolated hamster or rat liver mitochondria.[28] A positive correlation was identified between the antialcohol properties of daidzin (and its analogues) and the ability to increase 5-hydroxyindole-3-acetaldehyde concentrations in serotonin metabolism. Positive antialcohol effects required inhibition of ALDH2 but no inhibition of monoamine oxidase. These results suggest that the increase in concentration of biogenic aldehydes derived from the action of MAO may mediate the antidipsotropic action of daidzin. This has led to the design of daidzin analogues that have potent inhibition against ALDH2 but no activity against MAO.[29] The involvement of biogenic aldehydes may explain physiological studies that daidzin suppresses the voluntary intake of alcohol

[§] The PDB code for the coordinates of the complex structure reported is 2vle.

* To whom correspondence should be addressed. Phone: +44 1865 275384. Fax: +44 1865 275 182. E-mail: edl@biop.ox.ac.uk.

[†] University of Oxford.

[‡] Centre for Biochemical and Biophysical Sciences and Medicine, Harvard Medical School.

[#] Department of Pathology, Harvard Medical School.

[a] Abbreviations: ALDH, mitochondrial aldehyde deyhdrogenase; DS, disulfiram.

10.1021/jm800488j CCC: $40.75
Published on Web 07/10/2008

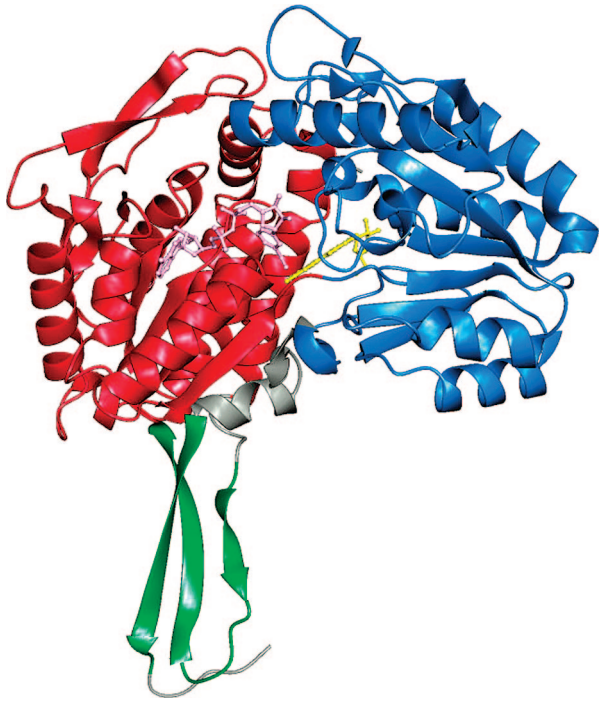

Figure 1. Structure of a subunit of human mitochondrial aldehyde dehydrogenase represented as a ribbon diagram and colored to indicate the domain structure of the protein. The coenzyme-binding domain is shown in red, the catalytic domain is shown in blue, and the oligomerization domain is shown in green. Residues 471−485, which do not fall into this domain nomenclature, are shown in gray. Daidzin is shown in yellow, bound into a deep pocket between the catalytic and the dinucleotide-binding domains. A molecule of bound NAD^+ is shown in pink bound in a cleft in the coenzyme-binding domain shown for reference, although NAD^+ was not included in the present structure. The figure was produced using the program AESOP (Noble, MEM; unpublished work).

in alcohol-preferring rats and is able to influence addictive behavior without entering the brain.[30]

Daidzin is the active principle of an ancient herbal remedy using the kudzu vine (*Peruraria lobata*) that has been used apparently safely and effectively for the treatment of "alcohol addiction" for over a millennium. The proof of principal experiments from the gene antisense studies[14] together with information that certain daidzin analogues are about to start in clinical trials and the need for new treatments for alcoholism[22] provided the motivation for us to describe our structural studies on daidzin binding to ALDH2.

Results and Discussion

Overview of the 3D Structure of ALDH2. The crystal structures of bovine and human ALDH2 have been described.[31,32] ALDH2 is a tetrameric enzyme comprising individual subunits of 500 amino acid residues. Each subunit consists of three domains. Two of these domains are based on the Rossmann fold for binding dinucleotides. One domain (comprising residues 8−135 and 159−270) binds the coenzyme NAD^+, and the other domain (comprising residues 271−470) is the catalytic domain that binds substrate (e.g., AcH). These two domains each contain a five-stranded α/β-dinucleotide-binding fold with an additional two-stranded β-sheet structure located above the strand equivalent to $\beta 3$ of a typical Rossmann fold. The third domain, referred to as the oligomerization domain, consists of a three-stranded β-sheet from residues 140−158 and 486−495 (Figure 1). NAD^+ binds in a cleft in the coenzyme-binding domain, making van der Waals contacts with residues Gly225, Pro226, Val249, and Leu252. In common with other NAD^+ binding proteins, ALDH2 utilizes a Rossmann fold in its interaction with the coenzyme, although the fold observed in ALDH2 differs slightly from the typical structure with unique features that have been described previously.[33]

Table 1. Summary of Crystallographic Data

data collected	ESRF ID14.EH1
space group	$P2_12_12_1$
unit cell (Å)	$a = 142.77$, $b = 151.00$, $c = 176.99$
resolution (highest range) (Å)	26.6−2.4 (2.46−2.4)
no. reflections	914 523
no. unique reflections	143 547
multiplicity	2.3
$I/\sigma(I)$	10.1 (4.7)
completeness (%)	96.3 (93.3)
R_{sym}	0.047 (0.146)
Wilson B factor (Å^2)	48.38
Refinement Statistics	
molecules per asymmetric unit	two tetramers
protein atoms	60344
waters	1405
R_{conv}	0.195
R_{free}	0.249
mean protein B factor (Å^2)	26.55
rmsd bond lengths (Å)	0.005
rmsd bond angles (deg)	0.604

Daidzin-Binding Site. Human ALDH2 was cocrystallized with daidzin and the structure of the complex solved to 2.4 Å (Table 1). The crystals are space group $P2_12_12_1$ and contain two copies of tetrameric ALDH2 in each asymmetric unit. Comparison with apo ALDH2[31] revealed a very similar structure. The overall root-mean-square difference of the daidzin complex from the apo ALDH2 structure is 0.28 Å for all α-carbon positions in a tetramer or 0.20 Å for a single monomer.

Daidzin is bound in a hydrophobic pocket formed in a cleft between the catalytic and dinucleotide-binding domains of all eight subunits in the asymmetric unit. The site is adjacent to the NAD^+ binding site[31,32] (Figure 1). The separations of the daidzin sites between one subunit and the others in the tetrameric protein are between 43 and 45 Å. The isoflavone ring structure makes extensive van der Waals contacts with surrounding residues including a long contact to Cys302 (Figure 2a). Cys302 has been identified as a key catalytic group.[34] The separation of the daidzin O4′-hydroxyl oxygen from the sulfur atom of Cys302 is 3.7 Å, and it is clear that there is no covalent interaction. Despite the overall similarity of the apo and daidzin ALDH2 structures, there is an induced localized change in conformation. The side chain of Cys302 shifts 2.5 Å away from the site in order to avoid a too close contact with the phenoxy O4′ ring of daidzin. In five of the eight subunits there is a hydrogen bond from the O4′-hydroxyl group of daidzin to an ordered water molecule, which in turn forms a hydrogen bond with Glu268, the general base residue important for catalysis[34] (Figure 2a). In the other three subunits, the Glu268 side chain is turned away from the daidzin-binding site. The structure shows that daidzin and substrate binding are mutually exclusive, consistent with results from kinetic studies that showed that daidzin inhibition is competitive with respect to the aldehyde substrate.[17]

A particularly striking feature of the daidzin/ALDH2 complex is packing of the daidzin planar isoflavone ring structure of between layers of the planar residue side chains (Phe170, Trp177, Phe296, and Phe459) (Figure 2b). Daidzin is almost 90% buried. The buried molecular surface area for daidzin is

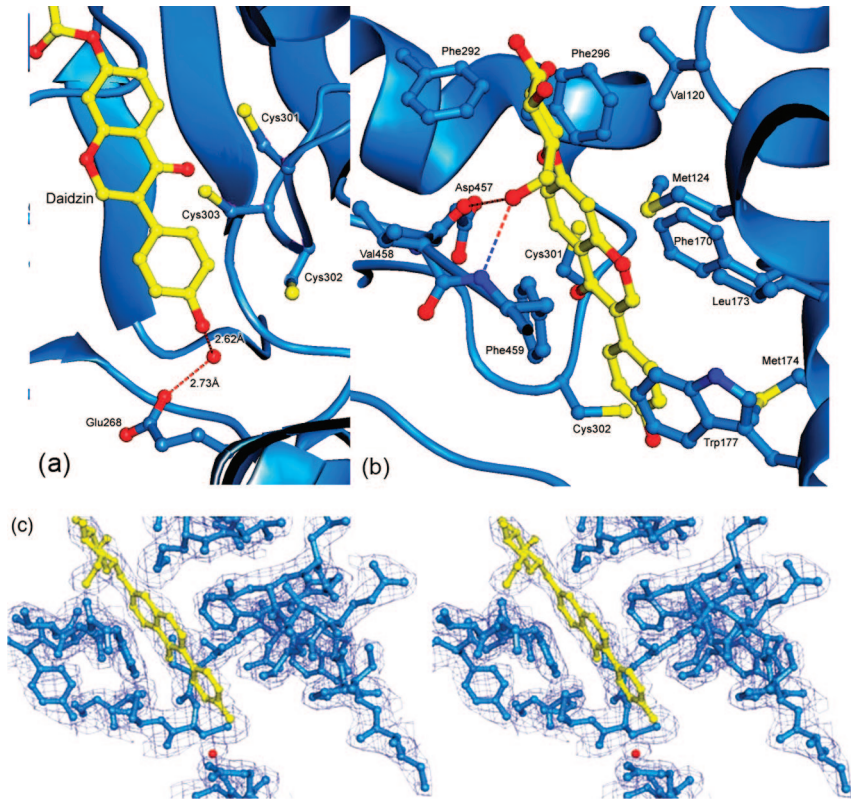

Figure 2. Interactions between ALDH2 and bound daidzin. (a) Details of the region around the 4′-OH of daidzin, showing the hydrogen-bonding network formed between the 4′-OH of daidzin and ordered water and Glu268. The side chains of the three catalytic site cysteine residues (Cys301, Cys302, and Cys303) are shown. This figure illustrates the binding observed in the A subunit. (b) Details of the isoflavone and glucosyl binding regions of the daidzin-binding site. The backbone of ALDH2 is shown as a ribbon diagram with the side chains of those residues forming contacts with daidzin. The planar residues Phe170, Trp177, Phe296, and Phe459 can be seen packing on either side of the planar isoflavone ring structure. (c) Refined electron density is shown in stereo for the region immediately surrounding bound daidzin, with the $2F_o - F_c$ map contoured at a level corresponding to 1σ. The figure was produced using the program AESOP (Noble, MEM; unpublished work).

344 Å^2 (from a total surface area 393 Å^2), and the surface area buried on ALDH2 is 379 Å^2, giving a total buried molecular surface area of 723 Å^2.

The CH groups from the C1, C3, and C5 carbons of the glucosyl ring pack against Val120, and C1 makes an additional contact to Phe296 while the CH group from C2 contacts Phe292 (Figure 2b). These interactions are typical of protein carbohydrate interactions that exploit the hydrophobic face of the glucosyl ring,[35] but there are no carbohydrate/aromatic group packing interactions. However, in contrast to most carbohydrate protein interactions there are no hydrogen bonds to the O2, O3, and O4 hydroxyl groups. Only the O6 hydroxyl makes a hydrogen bond. The other polar groups are exposed to the solvent. In all eight subunits the O6-hydroxyl hydrogen bonds to the carbonyl O of Asp457 (an average bond distance of 2.8 Å across all subunits) and the main-chain N of Phe459 (an average bond distance of 2.8 Å across all subunits) (Figure 2b).

NAD$^+$ Binding Site. The daidzin binding pocket is distinct from but adjoins the NAD$^+$ binding site in the coenzyme-binding domain (Figure 1). The structure of the ALDH2/NAD$^+$ complex[31] has shown that NAD$^+$ can bind to ALDH2 in two distinct conformations. Superposition of the structure of ALDH2/daidzin with that of the ALDH2/NAD$^+$ complex suggests that steric clashes would occur between one of the conformations of NAD$^+$ (that seen bound to chains B, C, and G of the structure with PDB accession code 1CW3) and both Cys302 in its new conformation and the 4′-hydroxyl group of daidzin. The clashes would prevent simultaneous binding of both NAD$^+$ and daidzin. However, the other conformation of NAD$^+$ (that seen bound to chains A, D, E, F, and H) does not result in clashes between daidzin and NAD$^+$. NMR, fluorescence, and structural studies have shown that ALDH-bound NAD$^+$ has considerable conformational flexibility.[36,37] This suggests that the coenzyme could have the flexibility to assume another conformation that may avoid potential clashes and allow the formation of an enzyme/coenzyme/inhibitor ternary complex. Previous observations have shown that daidzin is not competitive with respect to NAD$^+$.[17]

Table 2. Inhibition of Hamster Liver ALDH2 by Daidzin and Daidzin Analogues (From Ref 29)

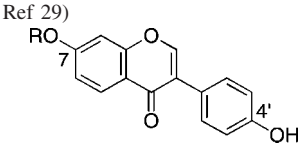

compd, R	IC_{50}, μM
1, Glc− (daidzin)	0.08
2, H− (daidzein)	9
3, CH_3− (prunetin)	0.45[a]
4, CH_3CH_2−	0.08
5, $CH_3(CH_2)_5$−	1.5
6, $CH_3(CH_2)_{11}$−	≫9
7, $HOOCCH_3$−	1.2
8, $HOOC(CH_2)_4$−	0.1
9, $HOOC(CH_2)_7$−	0.04
10, $HOOC(CH_2)_9$−	0.05
11, $HOOC(CH_2)_{10}$−	0.04
12, $HOOC(CH_2)_{11}$−	0.13
13, $H(OCH_2CH_2)_3$−	0.04

[a] K_i from ref 38.

Structural Analogues of Daidzin. Isoflavonoid derivatives, including prunetin (4′,5-dihydroxy-7-methoxyisoflavone), have

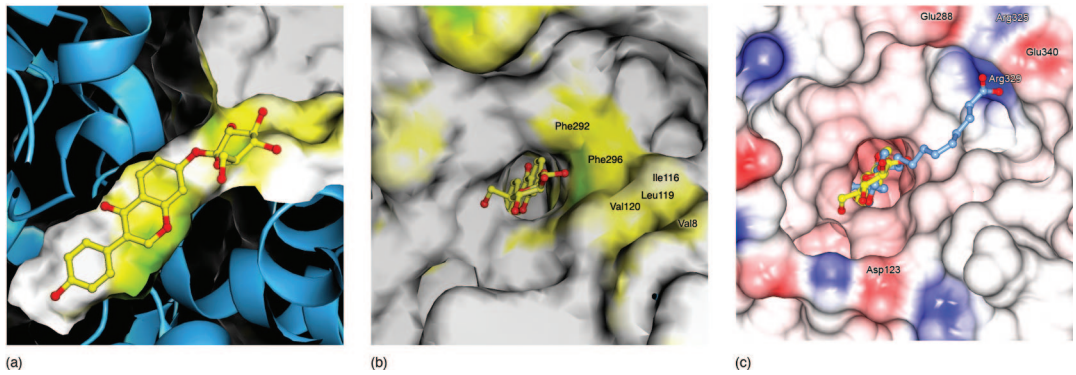

Figure 3. Surface representations of ALDH2 in the vicinity of bound daidzin: (a) substrate-binding site; (b) region immediately outside the substrate-binding site. Parts a and b are colored according to the hydrophobic potential calculated by GRID.[48,49] The deepest hydrophobic potential is colored green, the medium is yellow, and the neutral surface is white. The positions of the solvent exposed residues contributing to the external hydrophobic patch are indicated in part b. Parts a and b were produced using the program AESOP (Noble, MEM; unpublished work). (c) The same view as part b but with the molecular surface colored according to electrostatic potential as calculated using CCP4MG.[50] A model of compound **10** (Table 2, $HOOC(CH_3)_9-$ substituent, $IC_{50} = 0.05\ \mu M$), is shown in pale-blue, illustrating how the aliphatic chain may pack into a hydrophobic groove on the surface of ALDH2 and form polar contacts with two surface exposed residues Arg325 and Arg329.

been shown to be inhibitors of ALDH2. In kinetic studies with prunetin it was observed that prunetin does not displace bound NADH from an ALDH2/NADH complex,[38] consistent with the structural results that show daidzin and NAD^+ sites are distinct. However, the report that prunetin binds to only one subunit per tetramer is not supported by the structural results, which show that daidzin binds to all four subunits.

Structure−activity relationship studies for over 50 daidzin analogues have indicated structural features that are important for ALDH2 inhibition.[17,28,29] First, the 4′-OH function needs to be free. The structure gives an explanation for the requirement of a free 4′-OH group. The steric environment around the 4′-OH position excludes a daidzin analogue with a larger group substituted at this position. Although the hydroxyl group does not itself make a direct contact with the protein, in most of the subunits it is within hydrogen bonding distance of an ordered water molecule, with the distance varying between 2.5 and 2.8 Å. This water is within hydrogen-bonding distance of Glu268, thus establishing a hydrogen-bonding network that would act to stabilize the binding of compounds with a free 4′-OH.

Second, the structure−activity studies have shown that the 7-O-position can be substituted with a number of straight-chain alkyls with terminal polar functions such as −OH, −COOH, or $-NH_2$. A summary of results are shown in Table 2.[29] The preference for an unbranched alkyl chain terminating in a polar group may be understood by examining the properties of the surface of ALDH2 in the region adjacent to the binding pocket of the catalytic site. The glucosyl moiety of daidzin packs against the start of an extended hydrophobic patch on the surface of ALDH2 immediately outside the binding pocket of the catalytic site (Figure 3a). The patch comprises residues Val8, Ile116, Leu119, Val120, Phe292, and Phe296 (Figure 3b). We have modeled compound **10** (Table 2, $HOOC(CH_3)_9-$ substituent, $IC_{50} = 0.05\ \mu M$) using energy minimization with a simulated annealing protocol in phenix.refine.[39] We find the alkyl side chain can readily be accommodated in the hydrophobic channel and the carboxyl group reaches a position where it could potentially make favorable polar interactions with residues Arg329 and Arg325 (Figure 3c). Assuming that the other daidzin analogues bind in a similar mode, although for larger side chains there is considerable flexibility, we can understand some of the structure−function relationships. A simple H substituent (daidzein, compound **2**) provides little hydrophobic packing, but prunetin (**3**) could pack a methyl group in the hydrophobic tunnel and the longer ethyl CH_3CH_2- compound (**4**) would have even better hydrophobic contacts allowing it to bind as well as daidzin. The longer compounds in this series would expose the terminal CH_3 groups to the solvent, creating an unfavorable environment and providing a possible explanation for their lower affinity. For the carboxyl series, the smallest compound $HCOOC-CH_3-$ (compound **7**) would place the carboxylate in the hydrophobic patch and hence give less favorable binding than CH_3CH_2- (compound **4**). Longer compounds, which allow the carboxylate to reach the surface, can be accommodated with little discrimination (compounds **9**−**11**). The longest compound **12** appears to have less affinity, and this may be because the longer chain no longer allows the formation of both polar and nonpolar contacts simultaneously, requiring either the loss of polar contacts or exposure of an aliphatic group to the solvent. Compound **13**, the triethyleneglycol substituent, can be accommodated within the channel with satisfactory contacts. The results indicate that the channel is relatively tolerant for a number of substituents, but there are limitations on the nature of the substituents if they are either too small or too long.

Comparison of Daidzin Binding to ALDH2 and ALDH1. In order to understand the specificity of daidzin for ALDH2 over ALDH1, we constructed a model of human ALDH1 from the structure of sheep liver ALDH1 (PDB accession code 1bxs)[40] using the SWISS-MODEL server.[41] The substrate-binding cleft of ALDH1 is larger than that of ALDH2, allowing space to bind the bulky substrate retinal. It has been suggested that the larger site may explain the specificity of disulfiram for ALDH1 over ALDH2.[40] In the case of daidzin, we observe that the larger substrate-binding site would result in fewer and less intimate contacts with daidzin in ALDH1 than those achieved in ALDH2. In particular, the substitution of Phe459 to Val may be significant, since in ALDH2 Phe459 stacks against the isoflavone rings of daidzin providing a favorable binding environment. The substitutions Met124 to Gly and Leu173 to Val would also enlarge the substrate-binding cleft and remove favorable interactions observed between ALDH2 and daidzin. Of the residues comprising the surface patch immediately adjacent to the substrate-binding cleft, Val8, Ile116, Val120, Glu123, and Arg329 are not conserved. In ALDH1 Val8 is replaced conservatively with Leu; however, the other substitutions are Ile116 to Asn, Val120 to Asn, Asp123 to Ala, and Arg329 to Tyr. Of these, the change of Val120 to Asn is likely to have the most impact on daidzin binding, since

it would remove a favorable packing contact between Val120 and CH group of C1, C3, and C5 of the daidzin glucosyl moiety. These differences may combine to explain why daidzin is less effective as an inhibitor of ALDH1.[17]

Conclusion

The structure of human mitochondrial ALDH2 in complex with daidzin demonstrates the binding mode of this inhibitory compound at the substrate catalytic site in proximity to residues Cys302 and Glu268 and explains its ability to inhibit ALDH2. The glucosyl moiety of daidzin binds to a hydrophobic patch immediately adjacent to the catalytic site. The chemical properties of this site provide an explanation for the affinities of a number of daidzin 7-O-substituted compounds. The structure provides guidance on how the glucosyl group might be substituted with other groups in order to produce compounds with superior pharmacokinetic properties to daidzin while preserving the potency and specificity of the lead compound. Recent structural studies[42,43] on the E487K ALDH2*2 variant show that loss of activity occurs by disruption of a hydrogen-bonding network that, in the native ALDH2, stabilizes both the coenzyme binding and catalytic sites. Binding of NAD^+ leads to reordering of the coenzyme binding site but only partial reordering of the catalytic site. Thus, loss of activity of the natural variant ALDH2*2 and inhibition by daidzin both exert their effects at the active site of the enzyme.

Experimental Section

Crystallization and Data Collection. Human ALDH2 was expressed in *E. coli* BL21 (DE3) pLysS transformed with plasmid pT7-7 containing the *hALDH2* gene[44] and purified on *p*-hydroxyacetophenone−Sepharose affinity[45] followed by a Sephadex G150 column. ALDH2 produced in this manner exhibits a single band on SDS−PAGE and a specific activity of >5 (μmol/min)/mg protein (pH 9.0). Crystals of human ALDH2 were grown in sitting drops containing ALDH2 10 mg mL^{-1}, 100 mM MES, pH 6.5, 100 mM guanidine-HCl, 3 mM dithiothreitol, 5% DMSO (v/v), 10% PEG 6000 (w/v), and 2 mM daidzin. Two crystal forms were obtained: one was $P2_1$ with cell dimensions $a = 101.27$ Å, $b = 176.46$ Å, $c = 102.27$ Å, and $\beta = 94.91°$, which corresponds closely with the cell observed in the published structure of human ALDH2. The other crystal form was orthorhombic $P2_12_12_1$ with cell dimensions $a = 142.77$ Å, $b = 150.99$ Å, $c = 176.98$ Å. Data were collected at ESRF beamline ID14.EH1. The $P2_1$ crystal form suffered from severe radiation damage, preventing the collection of a complete data set to high resolution. The $P2_12_12_1$ crystal form proved more robust, and all results refer to the 2.4 Å resolution data collected from these crystals. Statistics from data processing are presented in Table 1.

Molecular Replacement and Refinement. The structure was solved by molecular replacement using the program MOLREP[46] with human ALDH2 as the search model (PDB accession code 1CW3).[31] A solution was found containing two tetramers of ALDH2 in the asymmetric unit. Rigid body refinement was then carried out using REFMAC[47] treating the four small three β-strand domains composing the core of each tetramer (residues 138−159 and 485−500 of each subunit) as a single rigid body and treating the remainder of each subunit (residues 7−137 and 160−484, comprising the two dinucleotide-binding domains) as an independent rigid body. Following 20 cycles of rigid body refinement, the structure showed a crystallographic *R* value of 0.317 and a free *R* value of 0.304. At this stage in refinement, initial difference density maps showed clear positive density in all eight catalytic sites in the asymmetric unit. A molecule of daidzin was built into each active site, and restrained maximum likelihood refinement was carried using phenix.refine[39] with alternating cycles of rebuilding, resulting in a final crystallographic *R* value of 0.195 and a free *R* value of 0.249. The coordinates have been deposited with the PDB and given the accession code 2vle.

Acknowledgment. We thank Dr. Henry Weiner for providing the pT7-7 plasmid containing human ALDH2 gene. We thank the beamline scientists at ESRF station ID14.EH1 for their support in data collection. The support of Dr. Bert L. Vallee is warmly acknowledged.

References

(1) Ehrig, T.; Bosron, W. F.; Li, T. K. Alcohol and aldehyde dehydrogenase. *Alcohol Alcohol.* **1990**, *25*, 105–116.
(2) Goedde, H. W.; Agarwal, D. P. Pharmacogenetics of aldehyde dehydrogenase (ALDH). *Pharmacol. Ther.* **1990**, *45*, 345–371.
(3) Weiner, H.; Wang, X. Aldehyde dehydrogenase and acetaldehyde metabolism. *Alcohol Alcoh., Suppl.* **1994**, *2*, 141–145.
(4) Pietruszko, R. Aldehyde dehydrogenase (EC 1.2.1.3). *Biochem. Physiol. Subst. Abuse* **1989**, *1*, 89–127.
(5) Klyosov, A. A. Kinetics and specificity of human liver aldehyde dehydrogenases toward aliphatic, aromatic, and fused polycyclic aldehydes. *Biochemistry* **1996**, *35*, 4457–4467.
(6) Crabbe, J. C. Use of genetic analyses to refine phenotypes related to alcohol tolerance and dependence. *Alcohol.: Clin. Exp. Res.* **2001**, *25*, 288–292.
(7) Li, T. K. Pharmacogenetics of responses to alcohol and genes that influence alcohol drinking. *J. Stud. Alcohol.* **2000**, *61*, 5–12.
(8) Chen, Y. C.; Lu, R. B.; Peng, G. S.; Wang, M. F.; Wang, H. K.; Ko, H. C.; Chang, Y. C.; Lu, J. J.; Li, T. K.; Yin, S. J. Alcohol metabolism and cardiovascular response in an alcoholic patient homozygous for the ALDH2*2 variant gene allele. *Alcohol.: Clin. Exp. Res.* **1999**, *23*, 1853–1860.
(9) Harada, S.; Agarwal, D. P.; Goedde, H. W.; Tagaki, S.; Ishikawa, B. Possible protective role against alcoholism for aldehyde dehydrogenase isozyme deficiency in Japan. *Lancet* **1982**, *2*, 827.
(10) Higuchi, S. Polymorphisms of ethanol metabolizing enzyme genes and alcoholism. *Alcohol Alcohol., Supplement* **1994**, *2*, 29–34.
(11) Ohmori, T.; Koyama, T.; Chen, C. C.; Yeh, E. K.; Reyes, B. V., Jr.; Yamashita, I. The role of aldehyde dehydrogenase isozyme variance in alcohol sensitivity, drinking habits formation and the development of alcoholism in Japan, Taiwan and the Philippines. *Prog. Neuro-Psychopharmacol. Biol. Psychiatry* **1986**, *10*, 229–235.
(12) Agarwal, D. P.; Harada, S.; Goedde, H. W. Racial differences in biological sensitivity to ethanol: the role of alcohol dehydrogenase and aldehyde dehydrogenase isozymes. *Alcohol.: Clin. Exp. Res.* **1981**, *5*, 12–16.
(13) Yoshida, A.; Huang, I. Y.; Ikawa, M. Molecular abnormality of an inactive aldehyde dehydrogenase variant commonly found in Orientals. *Proc. Natl. Acad. Sci. U.S.A.* **1984**, *81*, 258–261.
(14) Ocaranza, P.; Quintanilla, M. E.; Tampier, L.; Karahanian, E.; Sapag, A.; Israel, Y. Gene therapy reduces ethanol intake in an animal model of alcohol dependence. *Alcohol.: Clin. Exp. Res.* **2008**, *32*, 52–57.
(15) Hald, J.; Jacobsen, E. A drug sensitising the organism to ethyl alcohol. *Lancet* **1948**, *255*, 1001–1004.
(16) Banys, P. The clinical use of disulfiram (Antabuse): a review. *J. Psychoact. Drugs* **1988**, *20*, 243–261.
(17) Keung, W. M.; Vallee, B. L. Daidzin: a potent, selective inhibitor of human mitochondrial aldehyde dehydrogenase. *Proc. Natl. Acad. Sci. U.S.A.* **1993**, *90*, 1247–1251.
(18) Shen, M. L.; Johnson, K. L.; Mays, D. C.; Lipsky, J. J.; Naylor, S. Determination of in vivo adducts of disulfiram with mitochondrial aldehyde dehydrogenase. *Biochem. Pharmacol.* **2001**, *61*, 537–545.
(19) Brewer, C.; Meyers, R. J.; Johnsen, J. Does disulfiram help to prevent relapse in alcohol abuse? *CNS Drugs* **2000**, *14*, 329–341.
(20) Kranzler, H. R. Pharmacotherapy of alcoholism: gaps in knowledge and opportunities for research. *Alcohol Alcohol.* **2000**, *35*, 537–547.
(21) Schuckit, M. A. Recent developments in the pharmacotherapy of alcohol dependence. *J. Consulting Clin. Psychol.* **1996**, *64*, 669–676.
(22) Miller, G. Tackling alcoholism with drugs. *Science* **2008**, *320*, 168–170.
(23) Keung, W. M.; Vallee, B. L. Daidzin and daidzein suppress free-choice ethanol intake by Syrian golden hamsters. *Proc. Natl. Acad. Sci. U.S.A.* **1993**, *90*, 10008–10012.
(24) Heyman, G. M.; Keung, W. M.; Vallee, B. L. Daidzin decreases ethanol consumption in rats. *Alcohol.: Clin. Exp. Res.* **1996**, *20*, 1083–1087.
(25) Lin, R. C.; Guthrie, S.; Xie, C. Y.; Mai, K.; Lee, D. Y.; Lumeng, L.; Li, T. K. Isoflavonoid compounds extracted from *Pueraria lobata*

suppress alcohol preference in a pharmacogenetic rat model of alcoholism. *Alcohol.: Clin. Exp. Res.* **1996**, *20*, 659–663.
(26) Overstreet, D. H.; Lee, Y. W.; Rezvani, A. H.; Pei, Y. H.; Criswell, H. E.; Janowsky, D. S. Suppression of alcohol intake after administration of the Chinese herbal medicine, NPI-028, and its derivatives. *Alcohol.: Clin. Exp. Res.* **1996**, *20*, 221–227.
(27) Keung, W. M.; Lazo, O.; Kunze, L.; Vallee, B. L. Daidzin suppresses ethanol consumption by Syrian golden hamsters without blocking acetaldehyde metabolism. *Proc. Natl. Acad. Sci. U.S.A.* **1995**, *92*, 8990–8993.
(28) Rooke, N.; Li, D. J.; Li, J.; Keung, W. M. The mitochondrial monoamine oxidase−aldehyde dehydrogenase pathway: a potential site of action of daidzin. *J. Med. Chem.* **2000**, *43*, 4169–4179.
(29) Gao, G. Y.; Li, D. J.; Keung, W. M. Synthesis of potential antidipsotropic isoflavones: inhibitors of the mitochondrial monoamine oxidase−aldehyde dehydrogenase pathway. *J. Med. Chem.* **2001**, *44*, 3320–3328.
(30) Benlhabib, E.; Baker, J. I.; Keyler, D. E.; Singh, A. K. Kudzu root extract suppresses voluntary alcohol intake and alcohol withdrawal symptoms in P rats receiving free access to water and alcohol. *J. Med. Food* **2004**, *7*, 168–179.
(31) Ni, L.; Zhou, J.; Hurley, T. D.; Weiner, H. Human liver mitochondrial aldehyde dehydrogenase: three-dimensional structure and the restoration of solubility and activity of chimeric forms. *Protein Sci.* **1999**, *8*, 2784–2790.
(32) Steinmetz, C. G.; Xie, P.; Weiner, H.; Hurley, T. D. Structure of mitochondrial aldehyde dehydrogenase: the genetic component of ethanol aversion. *Structure* **1997**, *5*, 701–711.
(33) Liu, Z. J.; Sun, Y. J.; Rose, J.; Chung, Y. J.; Hsiao, C. D.; Chang, W. R.; Kuo, I.; Perozich, J.; Lindahl, R.; Hempel, J.; Wang, B. C. The first structure of an aldehyde dehydrogenase reveals novel interactions between NAD and the Rossmann fold. *Nat. Struct. Biol.* **1997**, *4*, 317–326.
(34) Weiner, H.; Farres, J.; Rout, U. J.; Wang, X.; Zheng, C. F. Site directed mutagenesis to probe for active site components of liver mitochondrial aldehyde dehydrogenase. *Adv. Exp. Med. Biol.* **1995**, *372*, 1–7.
(35) Johnson, L. N.; Cheetham, J.; McLaughlin, P. J.; Acharya, K. R.; Barford, D.; Phillips, D. C. Protein−oligosaccharide interactions: lysozyme, phosphorylase, amylases. *Curr. Top. Microbiol. Immunol.* **1988**, *139*, 81–134.
(36) Hammen, P. K.; Allali-Hassani, A.; Hallenga, K.; Hurley, T. D.; Weiner, H. Multiple conformations of NAD and NADH when bound to human cytosolic and mitochondrial aldehyde dehydrogenase. *Biochemistry* **2002**, *41*, 7156–7168.
(37) Perez-Miller, S. J.; Hurley, T. D. Coenzyme isomerization is integral to catalysis in aldehyde dehydrogenase. *Biochemistry* **2003**, *42*, 7100–7109.
(38) Sheikh, S.; Weiner, H. Allosteric inhibition of human liver aldehyde dehydrogenase by the isoflavone prunetin. *Biochem. Pharmacol.* **1997**, *53*, 471–478.
(39) Adams, P. D.; Grosse-Kunstleve, R. W.; Hung, L. W.; Ioerger, T. R.; McCoy, A. J.; Moriarty, N. W.; Read, R. J.; Sacchettini, J. C.; Sauter, N. K.; Terwilliger, T. C. PHENIX: building new software for automated crystallographic structure determination. *Acta Crystallogr. D* **2002**, *58*, 1948–1954.
(40) Moore, S. A.; Baker, H. M.; Blythe, T. J.; Kitson, K. E.; Kitson, T. M.; Baker, E. N. Sheep liver cytosolic aldehyde dehydrogenase: the structure reveals the basis for the retinal specificity of class 1 aldehyde dehydrogenases. *Structure* **1998**, *6*, 1541–1551.
(41) Arnold, K.; Bordoli, L.; Kopp, J.; Schwede, T. The SWISS-MODEL workspace: a Web-based environment for protein structure homology modelling. *Bioinformatics* **2006**, *22*, 195–201.
(42) Larson, H. N.; Weiner, H.; Hurley, T. D. Disruption of the coenzyme binding site and dimer interface revealed in the crystal structure of mitochondrial aldehyde dehydrogenase "Asian" variant. *J. Biol. Chem.* **2005**, *280*, 30550–30556.
(43) Larson, H. N.; Zhou, J. Z.; Chen, Z. Q.; Stamler, J. S.; Weiner, H.; Hurley, T. D. Structural and functional consequences of coenzyme binding to the inactive Asian variant of mitochondrial aldehyde dehydrogenase. Roles of residues 475 and 487. *J. Biol. Chem.* **2007**, *282*, 12940–12950.
(44) Zheng, C. F.; Wang, T. T.; Weiner, H. Cloning and expression of the full-length cDNAS encoding human liver class 1 and class 2 aldehyde dehydrogenase. *Alcohol.: Clin. Exp. Res.* **1993**, *17*, 828–31.
(45) Ghenbot, G.; Weiner, H. Purification of liver aldehyde dehydrogenase by *p*-hydroxyacetophenone−Sepharose affinity matrix and the coelution of chloramphenicol acetyl transferase from the same matrix with recombinantly expressed aldehyde dehydrogenase. *Protein Expression Purif.* **1992**, *3*, 470–478.
(46) Vagin, A.; Teplyakov, A. MOLREP: an automated program for molecular replacement. *J. Appl. Crystallogr.* **1997**, *30*, 1022–1025.
(47) Murshudov, G. N.; Vagin, A. A.; Dodson, E. J. Refinement of macromolecular structures by the maximum-likelihood method. *Acta Crystallogr. D* **1997**, *53*, 240–255.
(48) Goodford, P. Multivariate characterization of molecules for QSAR analysis. *J. Chemom.* **1996**, *10*, 107–117.
(49) Goodford, P. J. A computational-procedure for determining energetically favorable binding-sites on biologically important macromolecules. *J. Med. Chem.* **1985**, *28*, 849–857.
(50) Potterton, L.; McNicholas, S.; Krissinel, E.; Gruber, J.; Cowtan, K.; Emsley, P.; Murshudov, G. N.; Cohen, S.; Perrakis, A.; Noble, M. Developments in the CCP4 molecular-graphics project. *Acta Crystallogr., Sect. D: Biol. Crystallogr.* **2004**, *60*, 2288–2294.

JM800488J